An ab Initio, Infrared, and Raman Investigation of Phosphate Ion Hydration

Cory C. Pye*,‡ and Wolfram W. Rudolph†

Department of Chemistry, Saint Mary's University, Halifax, Nova Scotia B3H 3C3, Canada, and Medizinische Fakultaet der TU Dresden, Institut fuer Virologie im MTZ, Technical University of Dresden, Fetscherstrasse 40, D-01307 Dresden, Germany

Received: June 5, 2003; In Final Form: July 28, 2003

The low-frequency infrared and Raman spectra of sodium and potassium phosphate solutions have been measured and discussed. The geometries, energies, and vibrational frequencies of various isomers of $PO_4^{3-}(H_2O)_n$, $n = 0-6$ are calculated at various levels up to MP2/6-31+G*. These properties are studied as a function of increasing cluster size. The experimental and theoretical vibrational spectra are compared.

1. Introduction

A basic understanding of the solvation properties of ions is essential to understand the properties of electrolyte solutions. For the ubiquitous solvent molecule water, analysis of X-ray and neutron diffraction data clearly demonstrates the concept of hydration shell.[1] This concept, as applied to metal ions, is also supported by Raman spectroscopy and ab initio calculations.[2,3] To support the authors' investigations into sulfato complex formation, a study of sulfate hydration was carried out,[4] in which the same shell idea is preserved. The biologically relevant phosphate ion is isoelectronic to sulfate ion and should possess similar features; however, a search of the literature of the past decade did not reveal any ab initio study of this important fundamental ion. The high charge on the naked phosphate suggests that this species will not be stable in the gas phase; however, it is undeniable that phosphate does exist in solution at high pH. Naked sulfate has the same problems, and at least three waters are needed to stabilize this ion against electron loss.[4] Nevertheless, ab initio modeling using restricted Hartree−Fock theory with modest basis sets, for the purposes of modeling the solution, gives reasonable values for structural and vibrational properties even without sufficient water.[4] In the same spirit, we present our studies of naked and hydrated phosphate ion including optimization and frequency calculation up to the MP2/6-31+G* levels and with up to six waters.

2. Method

Calculations were performed using Gaussian 92[6] utilizing the 6-31G*[7] and 6-31+G*[8] basis sets. The MP2 calculations utilize the frozen core approximation. The geometries were optimized using a stepping stone approach, in which the geometries at the levels HF/STO-3G, HF/3-21G, HF/6-31G*, MP2/6-31G*, HF/6-31+G*, and MP2/6-31+G* were sequentially optimized. For the related sulfate ion, larger basis sets did not lead to significant improvement, and the same is to be expected here. Default optimization specifications (rms/maximum displacement smaller than 0.0003/0.000 45 au, rms/maximum force smaller than 0.0012/0.0018 au) were normally used. After each level, where possible, a frequency calculation was performed at the same level, and the resulting Hessian was used in the following optimization. **Z**-matrix coordinates constrained to the appropriate symmetry were used to speed up the optimizations. Because frequency calculations are done at each level, any problems with the **Z**-matrix coordinates would manifest themselves by giving imaginary frequencies corresponding to modes orthogonal to the spanned **Z**-matrix space. The Hessian was evaluated at the first geometry (opt=CalcFC) for the first level in a series to aid geometry convergence. For brevity, we refer to 6-31G* as basis set A and 6-31+G* as B. Incremental binding energies were corrected for basis-set superposition error (BSSE) by the standard Boys−Bernardi counterpoise scheme.

Details of the spectral measurement are described in ref 5 and need not be repeated here.

3. Results and Discussion

3.1. Experimental Vibrational Spectra of Alkali Phosphate Solutions. The "free", undistorted PO_4^{3-} ion of T_d symmetry has nine modes of internal vibration and spans the vibrational representation $\Gamma_{vib} = A_1 + E + 2T_2$. All modes are Raman active, but only the T modes are IR active. Although the phosphate ion should have a simple spectrum, there is much confusion in the literature over the assignment of the modes of tertiary phosphate (see Table 1). The disagreement could arise because of unstoichiometric product being used or observation of the Raman bands of the hydrolysis products. Phosphate ion partially reacts with water to form strongly alkaline solutions as $PO_4^{3-} + H_2O \rightleftharpoons HPO_4^{2-} + OH^-$. These alkaline solutions must not be contaminated with carbon dioxide present in air because this would react with hydroxide and shift the equilibrium. The literature uncertainty prompted one of us[5] to further investigate sodium and potassium phosphate solutions over a wide range of concentrations, including the supercooled hydrated melt. The results are summarized in Tables 2−4 and shown in Figures 1−4.

Our results confirm the tetrahedral symmetry of phosphate as indicated in earlier work of Simon and Schultze,[9] Preston and Adams,[16] and Mathieu and Jacques,[10] with some deviations in frequency value and depolarization ratio. The depolarization ratio obtained in ref 16 at 0.012 is much larger than our value of 0.001. For the remaining bands, we determined that $\rho = 0.75 \pm 0.02$, as expected. Exact values of these depolarization ratios are not given in the older literature. Hanwick and Hoffman[11]

* To whom correspondence should be addressed.
‡ Saint Mary's University.
† Technical University of Dresden.

10.1021/jp035594h CCC: $25.00
Published on Web 09/16/2003

TABLE 1: Raman Vibrational Data from Literature (Depolarization Ratio in Parentheses)

cation	concn	$\nu_2(E)$	$\nu_4(T_2)$	$\nu_1(A_1)$	$\nu_3(T_2)$	ref
Na	23%	420	557	938	1025	9
K	33%	420	562	937	1022	
K	50%	419 (0.85)	560 (0.85)	939 (0.1)	1050 (IR)	10
K		420 (0.58)	573, 704 (0.71)	936 (0.19)	1014 (0.58)	11
		363	515	980	1082	12
		358	500	970	1080	13
	v. dil.			989		15
Na, K	0.005−4.0 M	412	550	934 (0.023)	1007 (0.93)	16

TABLE 2: Raman Frequencies (cm^{-1}) of Aqueous K_3PO_4 Solutions[a]

		PO_4^{3-}						HPO_4^{2-}
c_0 (mol/L)	water/salt	$\nu_2(E)$	$\nu_4(T_2)$	$\nu_1(A_1)$	half-width	ρ	$\nu_3(T_2)$	$\nu_1(A_1)$
0.026	2135:1			936.5	27.5			991
0.074	750:1			936.5	25.5		1004	989
0.148	372:1			936.3	24		1006	990
0.37	148:1	414	558	936.2	24.5		1007	989
0.74	73:1	414	558	935.6	24	0.001	1008	990
1.85	28:1	414	558	935.2	22.5	0.001	1010	
2.60	19:1	414	554	935.0	23	0.001	1012	
3.70	12:1	412	554	933.4	22	0.003	1014	

[a] PO_4^{3-} $\nu_1(A_1)$ accuracy is $\pm$ 0.2 cm^{-1}. The 3.70 M solution has an asymmetry at 920 $\pm$ 10 cm^{-1}.

TABLE 3: Infrared Frequencies (cm^{-1}) of Concentrated Aqueous K_3PO_4 Solutions[a]

c_0	$\nu_4(T_2)$	$\nu_3(T_2)$
1.85	560	1008
2.60	562	1007
3.70	563	1005

[a] The 3.70 M solution has a low-frequency shoulder at 935 $\pm$ 10 cm^{-1}.

TABLE 4: Raman and Infrared Frequencies (cm^{-1}) of Aqueous Na_3PO_4 Solutions[a]

	PO_4^{3-}							HPO_4^{2-}	
c_0 (mol/L)	$\nu_2(E)$	$\nu_4(T_2)$	$\nu_1(A_1)$	half-width	ρ	$\nu_3(T_2)$	IR ν_{max}	$\nu_1(A_1)$	IR $\nu_4(E)$
0.012			936.5	25			1011	989	1080
0.030			936.5	25		1009	1010	990	1080
0.060	415	558	936.6	25	0.001	1008	1009	990	1080

[a] Infrared frequencies are denoted with IR.

found an additional band at 704 cm^{-1}, which probably stems from carbonate formed by absorption of carbon dioxide from the air by these alkaline solutions. In the standard works of Nakamoto[13] and Herzberg,[12] the frequencies given for phosphate are actually those of the hydrogen phosphate ion. Robinson[14] inferred the incorrect frequencies from ref 12. Baldwin and Brown[15] determined the phosphate content in dilute aqueous solutions with laser Raman spectroscopy and misassigned the band at 989 cm^{-1} to the phosphate totally symmetric stretch. In such dilute solutions, the predominant form (giving rise to this band) is the hydrolysis product HPO_4^{2-}.

Table 2 shows that the totally symmetric stretching frequency falls with increasing concentration. Extrapolation to zero concentration gives the limiting value $\nu_0 = 936.6 \pm 0.2$ cm^{-1}. This frequency corresponds to the frequency at infinite dilution, at which phosphate is surrounded only by water molecules and the specific cation influence is not present. The concentration dependence was not determined in ref 16, which may be due to the larger inaccuracies in the frequency determination (2 cm^{-1}). Our results also show that the ν_1 frequency of the phosphate in sodium phosphate solutions at moderate concentrations is higher than that of potassium phosphate solutions but that they coalesce at infinite dilution. Sodium phosphate is much less soluble than potassium phosphate at ambient temperatures, and thus higher concentrations cannot be studied. The specific cation effect was previously noted and explained for sulfate solutions.[17]

The infrared spectrum of potassium phosphate solutions is given in Figure 2. The concentration dependence of the IR-active vibrations is easy to observe (see Table 3). In more dilute solutions, the vibration ν_4 of the hydrolysis product HPO_4^{2-} appears as a shoulder at 1080 $\pm$ 4 (see Figure 3), which increases with increasing dilution to become the most intense band. Simultaneously in the Raman spectrum, the ν_1 band increases in intensity (Figure 1). In the IR spectra of concentrated solutions, the concentration of the hydrolysis product is too small to give rise to a noticeable shoulder.

The apparent value of the peak maximum of $\nu_3(PO_4^{3-})$ shifts with increasing dilution to smaller wavenumber because of the increasing overlap with the tails of the water librations. Subtracting the water background gives the true frequency value of the peak maximum (Figure 4).

3.2. Concentrated K_3PO_4 Solutions and the Hydrated Melt. In highly concentrated solutions (1:12 K_3PO_4/H_2O), the tetrahedral symmetry of PO_4^{3-} is disturbed and the ν_1 vibration becomes infrared-active (see Table 3, Figure 4), which was noted before but not interpreted.[18] In the supercooled hydrated melt (1:8) and in the 3.70 M K_3PO_4, a clear low-frequency asymmetry of the ν_1 band is noticed. In the hydrated melt, the depolarization ratio is also higher than that in the dilute solutions. The water content of these solutions or melt is not sufficient to hydrate all of the ions, and the formation of contact ion pairs is possible. The T_2 modes lose degeneracy to become either $A_1 + E$ for mono- or tridentate C_{3v} or $A_1 + B_1 + B_2$ for bidentate C_{2v}. All are infrared and Raman-allowed, and the A_1 band is polarized. Because of the large half-widths of the bands, splitting is observed neither in the Raman nor in the IR spectra. However, a low-frequency shoulder on ν_3 is observed in the IR spectra and is made more clear in the second derivative (Figure 4).

3.3. Ab Initio Calculations: General Description of Structures. *3.3.1. PO_4^{3-}.* The phosphate ion possesses T_d symmetry at all levels investigated. The structures of the phosphate clusters are essentially the same as the analogous sulfate clusters, so we refer readers to Figure 2 of ref 4. In addition, the STO-3G and 3-21G basis sets gave larger phosphorus−oxygen bond distances than calculations at the other levels. For these reasons, we only report these results for phosphate ion itself.

The geometries and vibrational frequencies of the phosphate ion are given in Table S2 of the Supporting Information. The P−O bond distances are about 0.08 Å longer than the corresponding S−O distances in sulfate. As with sulfate, the inclusion of correlation effects via MP2 calculations lengthens the P−O bond distance and lowers both the stretching and deformation frequencies. The magnitude of the changes induced by including correlation is essentially the same as that in sulfate. However, the changes induced by adding a diffuse function are greater, presumably because of the larger negative charge and the greater importance of diffuse functions in this case.

3.3.2. $PO_4^{3-}\cdot(H_2O)$. The modes of interaction of water with phosphate ion are expected to be similar to that of sulfate, and thus, we expect that the previous analysis of the sulfate would carry over to predict a C_{2v} phosphate structure. Indeed, the C_{2v}

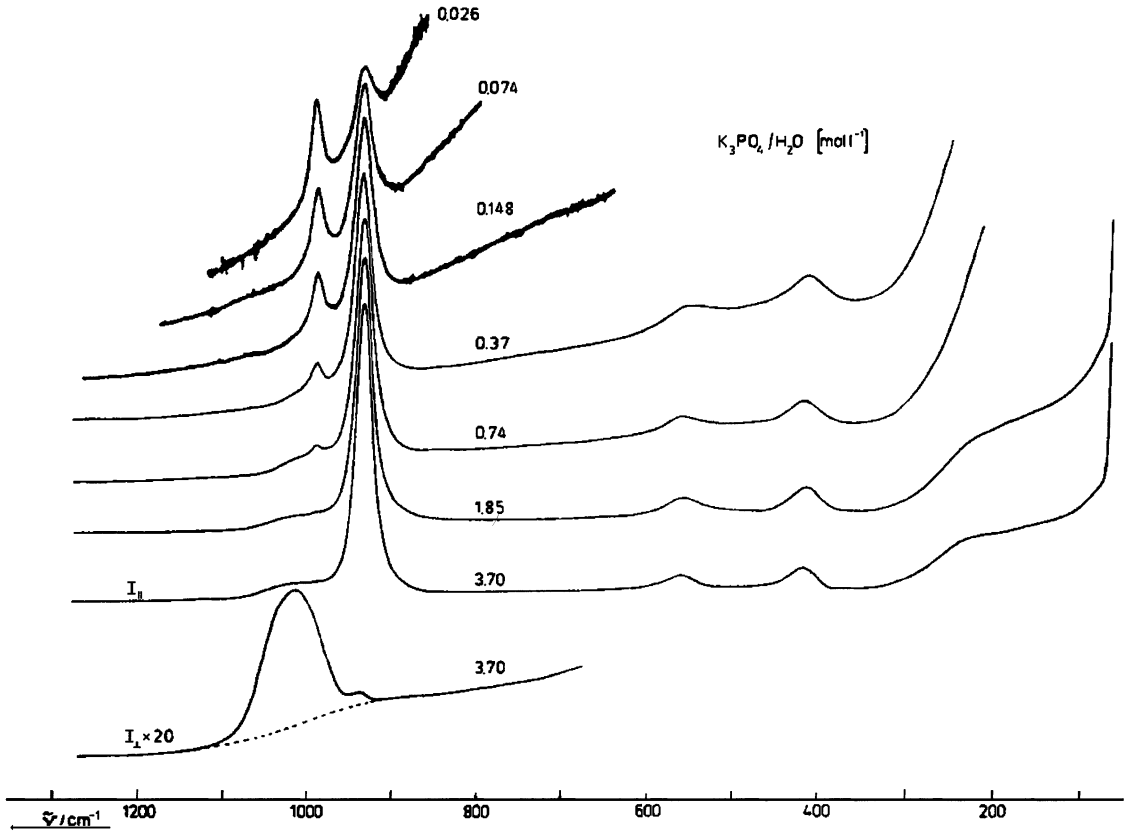

Figure 1. $I_\parallel$-Raman spectra (80−1280 cm^{-1}) of aqueous K_3PO_4 solutions in the concentration range 0.026−3.7 M. For the 3.7 M solutions, $I_\perp(20\times)$ is also shown.

structure has no imaginary frequencies at all levels above and including HF/3-21G.

Selected metrical parameters of the C_{2v} complex are given in Table S3 of the Supporting Information. The P−O(free) distance decreases relative to the uncomplexed phosphate, whereas the P−O(bound) distance increases. The hydrogen bonding weakens the P−O bond slightly, allowing the free P−O bond to strengthen. In the same way, the O−H distance is greater than that in the sulfate, and the hydrogen bond distance indicators are much shorter. The O···H distance is about 0.2 Å shorter and the O···O and P···O distances are about 0.1 Å shorter than those in the sulfate. This suggests that the hydrogen bonds to water are significantly stronger in the phosphate.

The frequencies of the complex are given in Table S4 of the Supporting Information. The water deformation modes increase by about 100−140 cm^{-1}, the water symmetric stretching modes decrease by about 500−700 cm^{-1}, and the water asymmetric stretching modes decrease by about 700−1100 cm^{-1}. These changes are much greater than those in the sulfate. The changes are more pronounced at the correlated level and are consistent with extreme weakening of the O−H bond. For the C_{2v} complex, the phosphate modes correlate as follows: $A_1 \rightarrow A_1$, $E \rightarrow A_1 + A_2$, and $T_2 \rightarrow A_1 + B_1 + B_2$. The $\nu_1(A_1)$ stretching mode is hardly affected by the coordinated water, whereas the $\nu_3(T_2)$ stretching mode splits significantly over a range of up to 130 cm^{-1}. The $\nu_2(E)$ deformation mode splits and is raised in frequency by up to 70 cm^{-1}, whereas the $\nu_4(T_2)$ deformation mode splits by 20 cm^{-1} but otherwise does not change. These changes mirror the changes in sulfate.

3.3.3. $PO_4^{3-}\cdot(H_2O)_2$. For sulfate, we previously established that only a single water will hydrogen bond to any given pair of oxygens. Phosphate is expected to behave similarly, and therefore, we did not calculate the C_{2v} dihydrate. The two remaining possibilities, D_{2d} and C_s, were calculated. The D_{2d} structure is the lowest in energy, followed closely (<4 kJ/mol) by the C_s structure (see Table 5). Differences in zero-point and thermal corrections to the enthalpy amount to less than 0.5 kJ/mol (MP2) or 0.1 kJ/mol (HF). We note that the isomers are energetically more separated than the corresponding sulfate species.

The metrical parameters of both species are given in Table S5 of the Supporting Information. The phosphorus−oxygen bond distances across the two isomers are similar and depend (to within ± 0.002 Å) only upon the number of hydrogen bonds each oxygen has. Each hydrogen bond lengthens the P−O distance by 0.020−0.029 Å, depending on level. The O−H distances are a little shorter when this donor hydrogen is hydrogen-bonded to a double-acceptor oxygen. The hydrogen-bonding indicators (O···H, O···O, P···O) show that the C_s and D_{2d} structures are very similar.

The frequencies of the two species are given in Tables S6 and S7 of the Supporting Information. Compared to the monohydrated phosphate, the OH stretching frequencies are higher by about 60−200 cm^{-1}, correlated levels giving a greater change. The bending modes are hardly affected by the additional water. The phosphate modes correspond as follows: for D_{2d}, $A_1 \rightarrow A_1$, $E \rightarrow A_1 + B_1$, $T_2 \rightarrow B_2 + E$; for C_s, $A_1 \rightarrow A'$, $E \rightarrow A' + A''$, $T_2 \rightarrow 2A' + A''$. Compared to the monohydrate, the modes are slightly increased in frequency. These trends are similar to sulfate, although the change in the OH stretching modes is about double that of the sulfate.

3.3.4. $PO_4^{3-}\cdot(H_2O)_3$. There are three possible structures for phosphate with three waters. Two of these have C_{3v} symmetry. One of these structures possesses a phosphate oxygen forming hydrogen bonds to three waters (#1), with each other oxygen forming one hydrogen bond. The other has one free oxygen

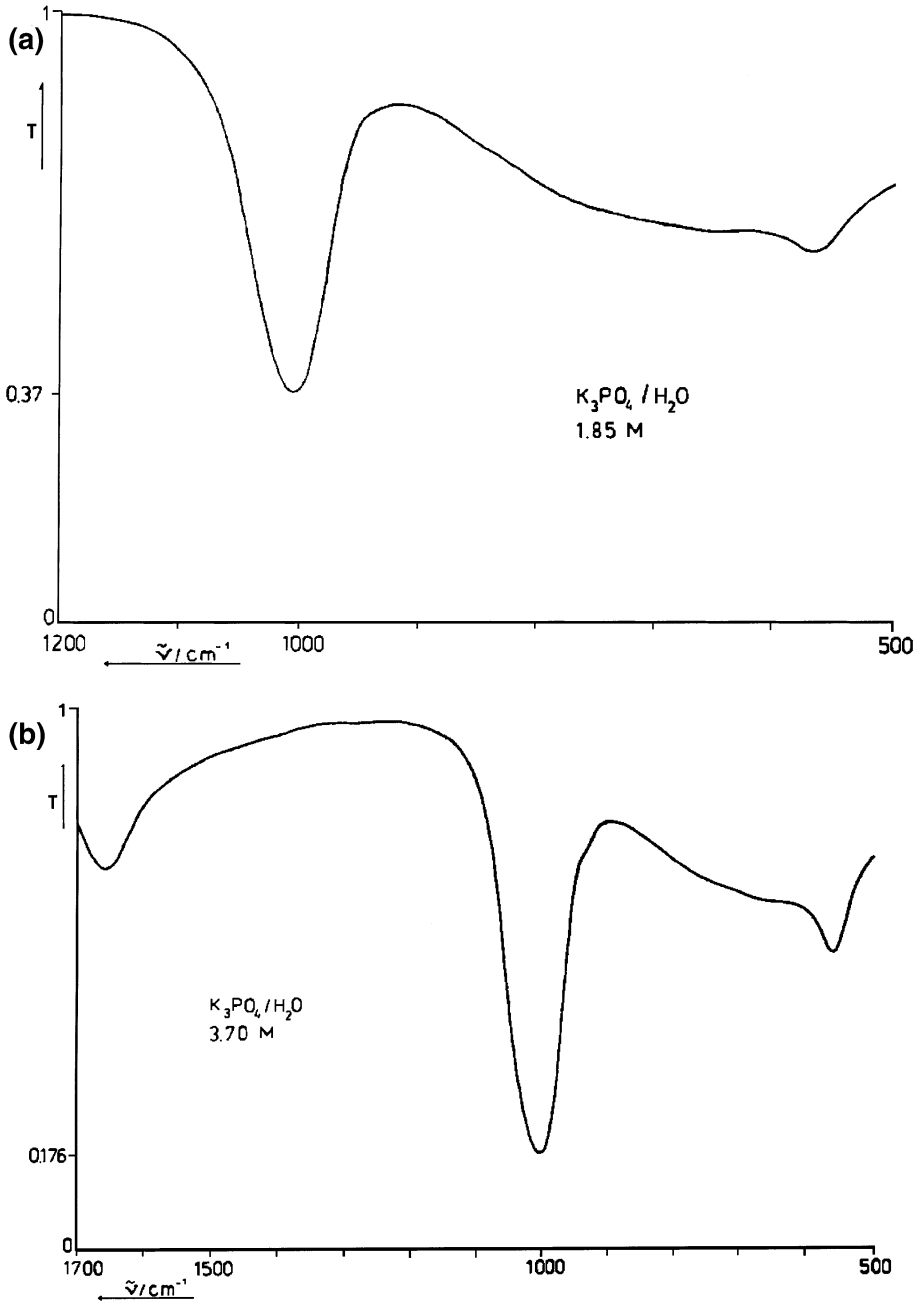

Figure 2. FT-IR spectrum of (a) 1.85 mol/L K_3PO_4 (500−1200 cm^{-1}) and (b) 3.70 mol/L K_3PO_4 (500−1700 cm^{-1}) (thin film, polyethylene-coated KBr disks).

and three oxygens having two hydrogen bonds (#2). There is also a C_2 structure possible. This last structure is electronically the most stable, the C_{3v} #2 structure being within 2.6 kJ/mol and the C_{3v} #1 within 3.8 kJ/mol (see Table 6). The difference in zero-point and thermal energy corrections between all structures is less than 0.4 kJ/mol.

The metrical parameters of all three species are given in Table S8 of the Supporting Information. The trends are similar to those for the diaqua species. For comparable hydrogen bonds, the OH distances in the triaqua are slightly shorter and may indicate some cooperative effects. The O···H distances increase with the more hydrogen bonds accepted by the oxygen atom.

The frequencies of all species are given in Tables S9, S10 and S11 of the Supporting Information. Compared to the dihydrated C_s phosphate, the OH stretching frequencies are higher by about 50−200 cm^{-1}, correlated levels giving a greater change. The bending modes are hardly affected by the additional water. The phosphate modes correspond as follows: for C_{3v}, $A_1 \rightarrow A_1$, $E \rightarrow E$, $T_2 \rightarrow A_1 + E$; for C_2, $A_1 \rightarrow A$, $E \rightarrow 2A$, $T_2 \rightarrow A + 2B$. Compared to the dihydrate, these modes are slightly increased in frequency.

3.3.5. $PO_4^{3-}\cdot(H_2O)_4$. The tetrahydrate may form either a C_s or D_{2d} structure. The D_{2d} structure is very slightly electronically favored by between 1.3 and 2.6 kJ/mol, depending on the level of theory. Differences between zero-point and temperature corrections are less than 0.1 kJ/mol.

The metrical parameters of both species are given in Table S12 of the Supporting Information. The trends are similar to those for the triaqua species. For comparable hydrogen bonds, those in the tetraaqua are slightly shorter and may indicate some cooperative effects.

The frequencies of all species are given in Tables S13 and S14 of the Supporting Information. We note that MP2/6-31+G* frequencies could not be carried out here because of computa-

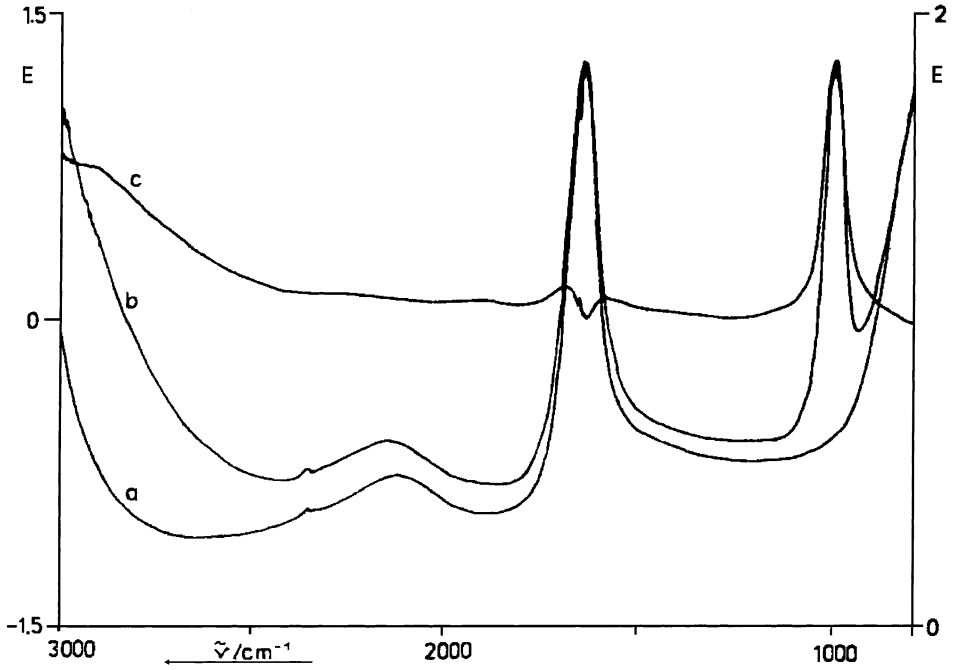

Figure 3. FT-IR spectra (800−3000 cm^{-1}, KRS-5 cuvette, 9 μm) of (a) water, (b) 0.592 mol/L aqueous sodium phosphate solution (right scale), and (c) difference between spectra a and b (left scale).

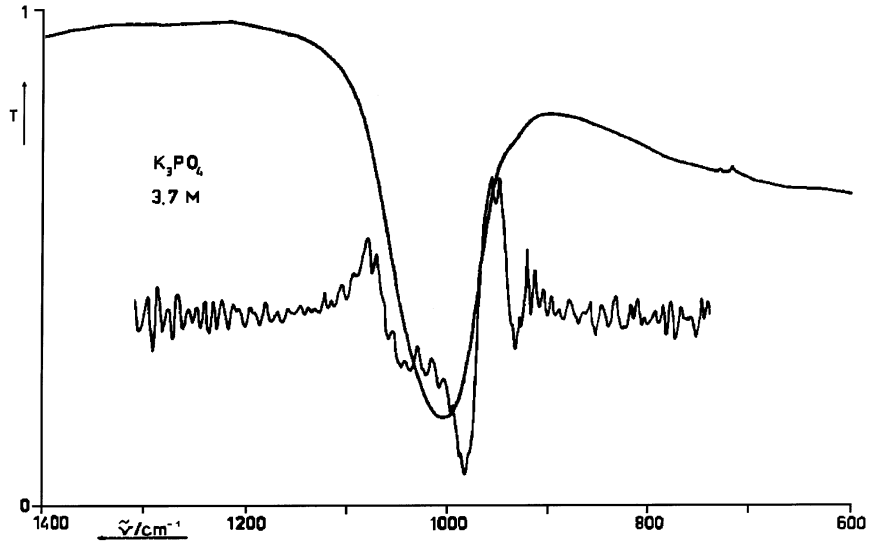

Figure 4. FT-IR spectrum of a 3.70 mol/L K_3PO_4 solution (thin film, polyethylene-coated KBr disks) and the negative second derivative (lower curve).

TABLE 5: Electronic Energies (kJ/mol) of C_s Isomer of $PO_4^{3-}\cdot(H_2O)_2$ Relative to D_{2d} Structure

level	energies
HF/A	3.2
HF/B	3.6
MP2/A	2.8
MP2/B	2.7

tional restrictions. Comparing the C_2 trihydrated phosphate with the D_{2d} tetrahydrated phosphate, the OH stretching frequencies are higher by about 100−150 cm^{-1}, correlated levels giving a greater change. The bending modes, as well as the phosphate modes, are slightly increased in frequency.

3.3.6. $PO_4^{3-}\cdot(H_2O)_5$. The only structure has symmetry C_{2v}. The metrical parameters are given in Table S15 of the Supporting Information. At the correlated levels, the O···H distance is slightly longer between comparable hydrogen bonds in the pentaaqua compared with the tetraaqua species.

TABLE 6: Electronic Energies (kJ/mol) of Other Isomers of $PO_4^{3-}\cdot(H_2O)_3$ Relative to C_2 Structure

	energies	
level	C_{3v} #1	C_{3v} #2
HF/A	3.4	2.0
HF/B	3.8	2.6
MP2/A	3.5	1.3
MP2/B	3.7	1.8

No correlated frequency calculations could be carried out for this structure. Compared to the tetraaqua D_{2d} structure, the symmetric OH stretching modes are increased by about 50 cm^{-1}, whereas the asymmetric modes are increased by about 80 cm^{-1}.

3.3.7. $PO_4^{3-}\cdot(H_2O)_6$. The only structure has symmetry T_d, and thus, we return to the symmetry of the naked phosphate itself. All of the hydrogen-bonding indicator distances are longer than those in the pentaaqua structure. The OH stretching modes

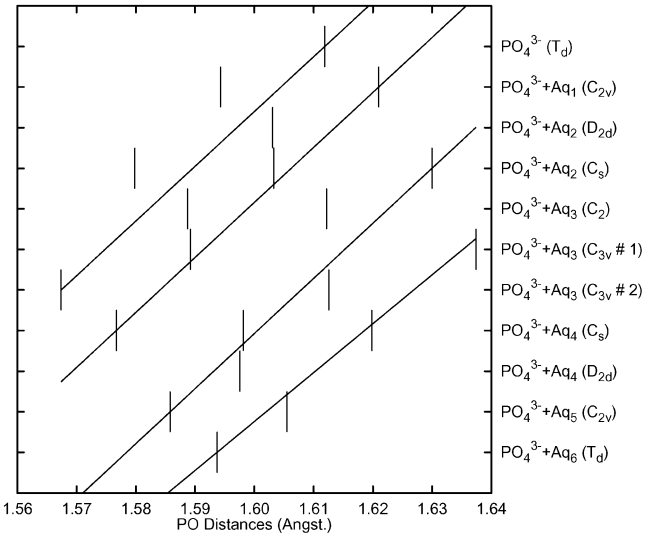

Figure 5. MP2/6-31+G* P−O distance in clusters.

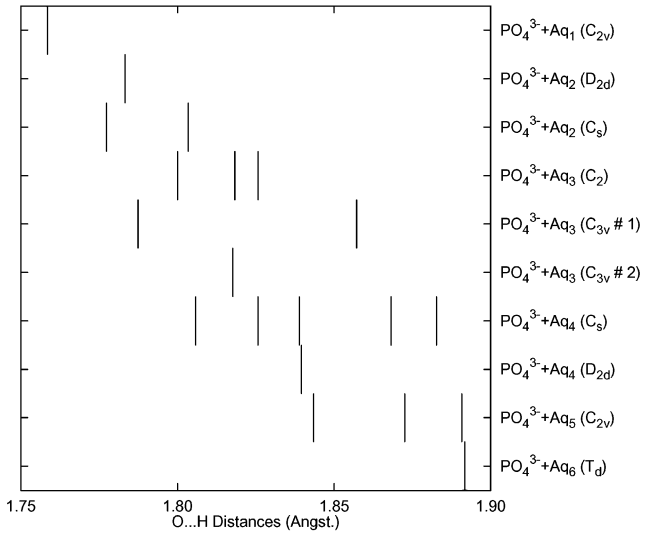

Figure 6. MP2/6-31+G* O···H distance in clusters.

are increased by about 20 cm^{-1}, whereas the asymmetric modes are increased by 70 cm^{-1}.

3.4. Discussion of Geometries. In Figure 5, we present the P−O distances in the phosphate ion itself as surrounded by various numbers of water molecules in various configurations. As with the sulfate, we can distinguish the P−O bonds by the number of hydrogen bonds that each oxygen accepts and connect them with lines. The more hydrogen bonds to an oxygen of phosphate, the longer the P−O bond distance will become. However, adding waters to the cluster shortens all other P−O bonds, and a partial cancellation results. Overall, the net effect is a shortening of the P−O distance between naked phosphate and its hexahydrate. The results are similar to the sulfate. The trends for the hydrogen-bonding indicators O···H (Figure 6), O···O (Figure 7), and P···O (Figure 8) is very clear; these distances lengthen as more waters hydrogen bond to the phosphate. This suggests that the hydrogen bonding becomes weaker as more waters bind to phosphate. The differences within a cluster, however, are more pronounced than those in the analogous sulfate cluster, a consequence of the stronger hydrogen bonding.

3.5. Discussion of Vibrational Frequencies. Figure 9 presents the vibrational frequencies of the clusters investigated at the HF/6-31+G* level. We note that, upon hydrating the

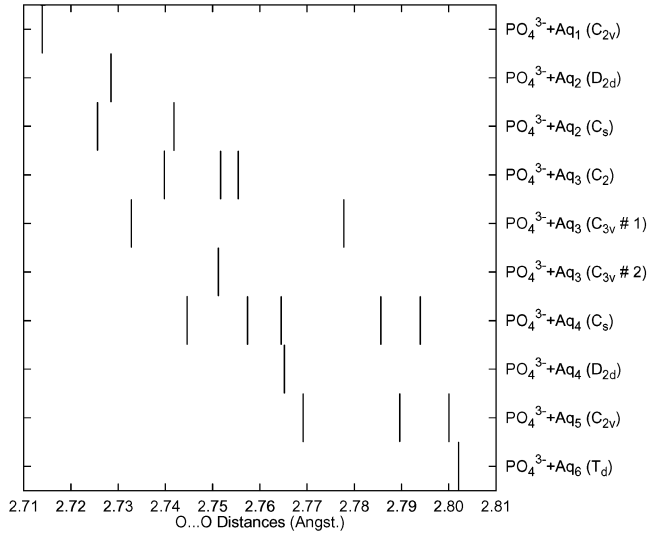

Figure 7. MP2/6-31+G* O···O distance in clusters.

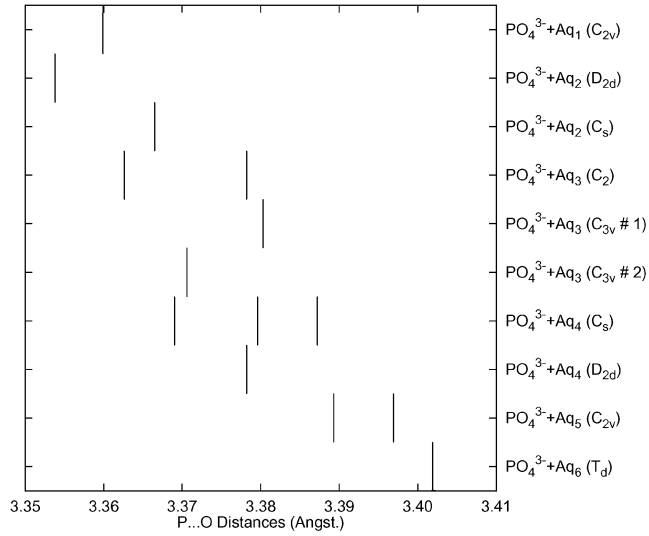

Figure 8. MP2/6-31+G* P···O distance in clusters.

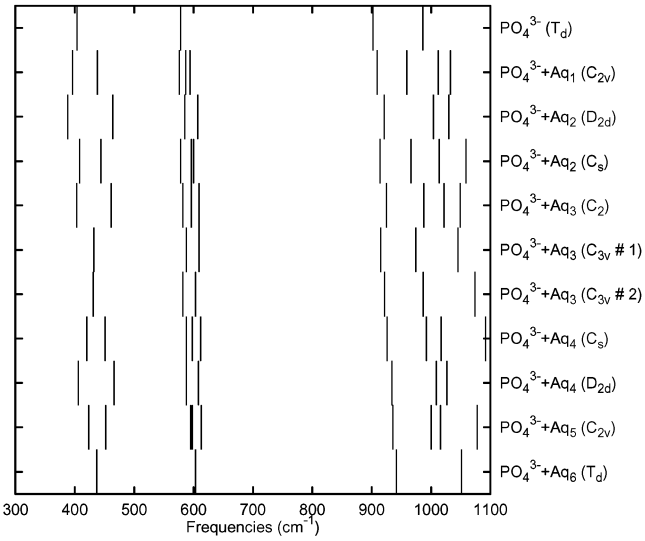

Figure 9. HF/6-31+G* phosphate mode frequencies in clusters.

phosphate ion with six waters, the frequencies increase by 25−40 cm^{-1}, with the exception of the $\nu_3(T_2)$ stretching mode, which increases by 65 cm^{-1}. This is in marked contrast to the

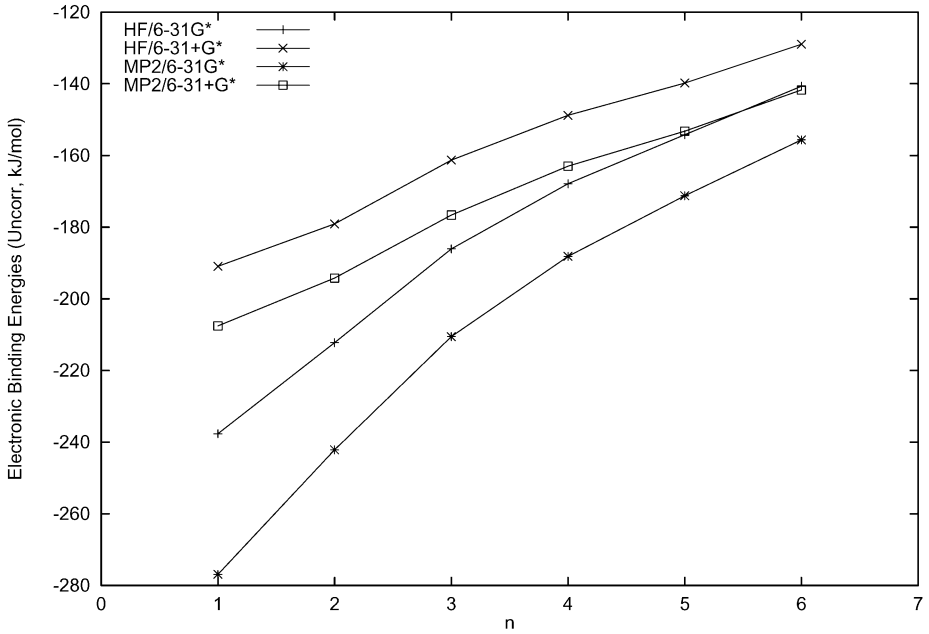

Figure 10. Phosphate incremental binding energies (uncorrected) for $PO_4^{3-}(H_2O)_{n-1} + H_2O \rightarrow PO_4^{3-}(H_2O)_n$.

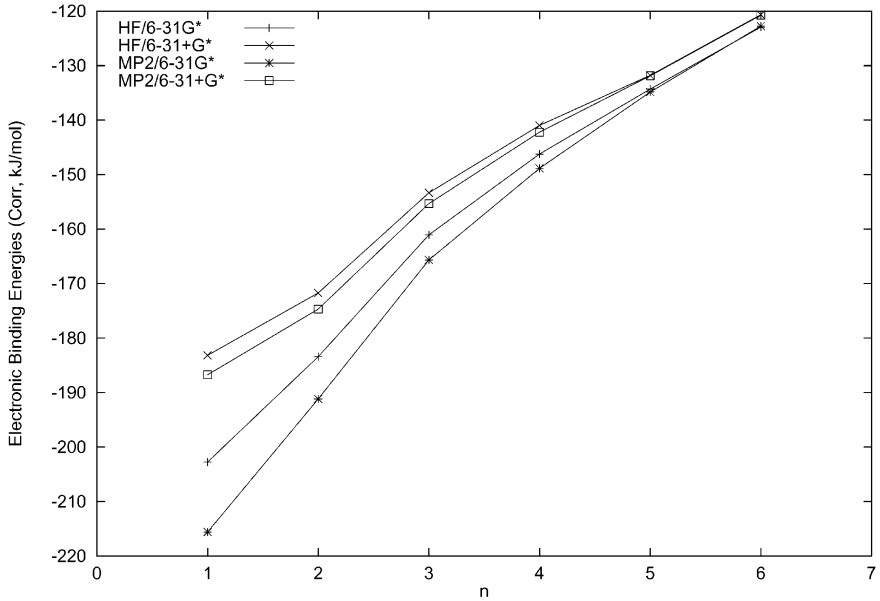

Figure 11. Phosphate incremental binding energies (corrected) for $PO_4^{3-}(H_2O)_{n-1} + H_2O \rightarrow PO_4^{3-}(H_2O)_n$.

sulfate, in which the increase was smaller and the ν_3 mode unexceptional. The experimental values of the frequencies of phosphate in water (as the potassium phosphate solution) are 414, 558, 936, and 1004 cm^{-1}. The Hartree−Fock calculation of the naked phosphate, except for ν_4, underestimates and that of the hexaaqua phosphate overestimates the vibrational frequency as compared to experiment. However, it is well-known that Hartree−Fock theory overestimates the frequencies and usually frequencies need to be scaled to account for both deficiencies in theory and neglect of anharmonic contributions. For the naked ion, we derived scaling factors for frequencies by linear regression. The Hartree−Fock values for basis sets A and B are 0.966 and 1.018 with standard errors of 0.021 and 0.014. The corresponding MP2 values are 1.054 and 1.172 with standard errors of 0.027 and 0.010, respectively. An improvement of the error when diffuse functions are added is noted, although the severe underestimation of the MP2/6-31+G* frequencies is obvious from the scale factor. For the hexahydrate, the HF/A and HF/B values are 0.952 and 0.962 with standard errors of 0.016 and 0.014. After scaling, the relative error with and without water is about the same for HF/6-31+G*. The naked phosphate ion has larger standard errors than the naked sulfate, possibly a consequence of the higher charge and the poorer electronic description. The relatively poor MP2/6-31+G* frequencies are noteworthy. These frequencies agree to within 10 cm^{-1} of the sophisticated B3LYP/6-311++G** calculations,[19] so the error is probably not due to the level of theory. In the same way, our experimental frequencies are within 10 cm^{-1} of a more recent Raman measurement.[20] In both of these cases, the largest outlier was ν_3, and with this point excluded, the remainder were within 4 cm^{-1}.

The experimental full widths at half-height (fwhh) were reported as 49, 52, 28.7, and 57 cm^{-1} in ref 20 for 0.067 mol/L sodium phosphate solutions at pH 14. Except for ν_3, these are greater than the corresponding sulfate half-widths from ref 4. From visual comparison of Figure 9 and the corresponding

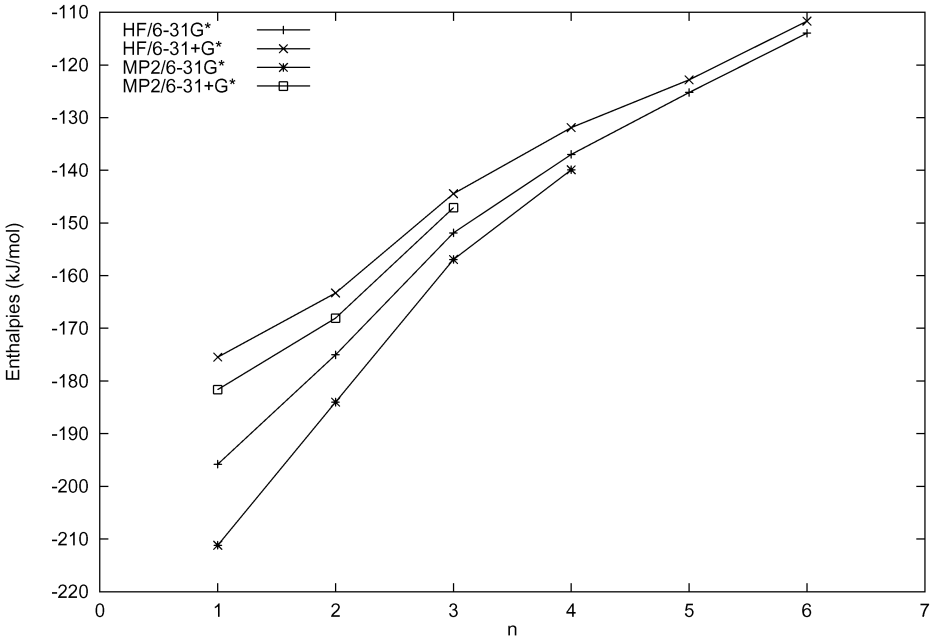

Figure 12. Phosphate incremental binding enthalpies for $PO_4^{3-}(H_2O)_{n-1} + H_2O \rightarrow PO_4^{3-}(H_2O)_n$.

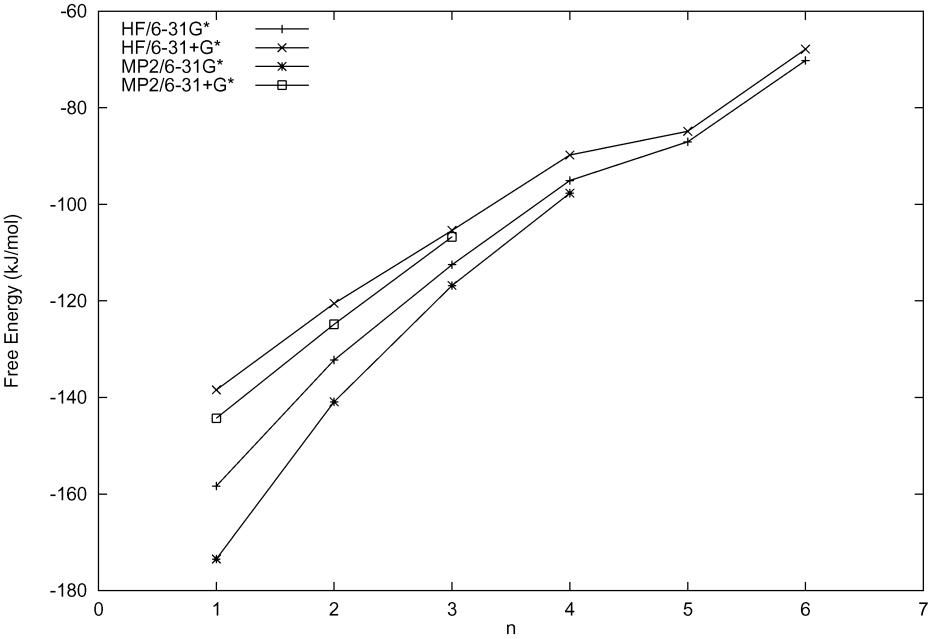

Figure 13. Phosphate incremental binding free energies for $PO_4^{3-}(H_2O)_{n-1} + H_2O \rightarrow PO_4^{3-}(H_2O)_n$.

Figure 7 in ref 4, we see that the theoretical degenerate mode splitting agrees with this observation. We may take all of the complexes from the mono- through to the pentaaqua clusters as a crude "sampling" of the phosphate solution environment at the HF/6-31+G* level. The average splitting is 36, 21, 0, and 68 cm^{-1}. The pentahydrate splitting is 29, 18, 0, and 78 cm^{-1}. The maximum splitting is 76, 27, 0, and 100 cm^{-1}. From this, we would expect that the half-widths of phosphate would all be greater than those of sulfate. Qualitatively, we have predicted that the half-width of ν_3 should be the greatest. The justification and interpretation of these half-widths are given in ref 4.

Theoretically, assuming a T_d model for phosphate or sulfate, we expect a depolarization ratio of zero for the $\nu_1(A_1)$ mode. In practice, totally symmetric modes give a small finite value. For phosphate, we obtained a value of around 0.001. For sulfate, a value of 0.005 was obtained. Although the exact value is very sensitive to the data treatment and difficult to establish, we suggest that this can be explained by the model in ref 4 as well. Any of the nonsymmetric model structures can give small nonzero depolarization ratios. The average values for phosphate and sulfate are 0.0026 and 0.0012, respectively. The pentahydrate values are 0.0001 and 0.0005. The maximum values are 0.0081 and 0.0027. We point out that different counterions and concentrations are used and that these should be regarded as order-of-magnitude estimates only.

3.6. Discussion of Binding Energies. The incremental binding energies of phosphate with water, uncorrected for BSSE effects, are given in Figure 10. A comparison of the results for the 6-31G* and 6-31+G* basis sets indicates a large effect of the diffuse functions on the binding energy with a larger effect at the correlated level. This suggests that the diffuse function is reducing the effect of BSSE and lowering the magnitude of the binding energy. The same pattern was observed for sulfate,

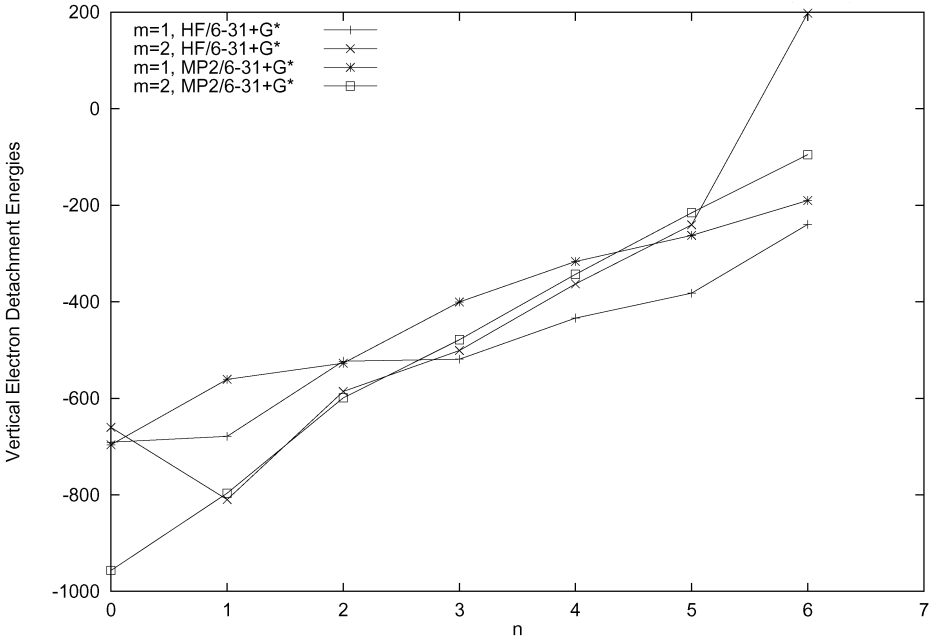

Figure 14. Phosphate vertical electron detachment energies for $PO_4^{3-}(H_2O)_n \rightarrow PO_4^{(3-m)-}(H_2O)_n + me^-$, $m = 1, 2$.

except that the basis set effect was more pronounced, resulting in the reversal of the HF/6-31G* and MP2/6-31+G* ordering. The binding energies are a little less than twice the sulfate values. This is indeed verified in the BSSE-corrected energies of Figure 11, in which the values are much more consistent across various levels, which suggests that the BSSE-free binding energy is not much affected by correlation energy. There is more of a spread in the values between the two basis sets. For highly charged systems such as phosphate, the importance of basis set relative to correlation increases. The binding enthalpies are given in Figure 12, and binding free energies in Figure 13. The clusters are destabilized, but the free energy is still very negative. These values are again slightly less than twice the value for sulfate, but use of the Born equation with the same radius would suggest a factor of $^9/_4 = 2.25$. The larger radius of phosphate (about 0.1 Å) is not enough to account for this difference and highlights the inadequacy of the crude Born model.

3.7. Discussion of Gas-Phase Stability. The phosphate ion, PO_4^{3-}, will not be stable with respect to electron loss. However, in aqueous solution at high pH, it is stable. A question that can be posed is how many waters are necessary to stabilize the ion. Although not critical for our purposes, it remains an interesting question, so we decided to investigate this crudely. With the optimized phosphate−water geometries of the most stable structure, at the appropriate levels, we performed single-point calculations of the corresponding mono- and dianion (see Table S19 of the Supporting Information). The difference in energy would correspond to the vertical one- or two-electron detachment energy. All structures were unstable with respect to electron loss to give the doublet dianion (See Figure 14). Only mild spin contamination was encountered (the difference between the projected and unprojected energies was about 0.01 au). For the singlet monoanion, more severe spin contamination is noted (0.1 au) and the energies are less reliable. It appears as though between three and five waters are required to stabilize the dianion relative to the monoanion. We may graphically estimate that if the trends continue, around nine waters should stabilize the phosphate ion from electron loss. It must be realized that this is a crude extrapolation and by no means certain. Future experiments with electrospray mass spectrometry and photoelectron spectroscopy, combined with theoretical calculations, for example, will hopefully soon answer these questions.

4. Conclusions

The Raman spectra of aqueous potassium and sodium phosphate has been measured. A series of ab initio calculations at several levels of theory on several hydrated phosphate moieties has been carried out, and structural, energetic, and vibrational characteristics have been determined. The vibrational frequencies as obtained from solution Raman measurements were reproduced after suitable scaling of the theoretical results for the unsolvated and hexasolvated sulfates. Some insight into the experimentally observed line widths of the degenerate modes was obtained by carrying out an analysis of the unsymmetric structures of the partially solvated clusters.

Acknowledgment. The authors thank the Computing and Communications Department, Memorial University of Newfoundland, for computer time and Richard D. M. Alfred, Center for Academic Technologies, Saint Mary's University, for graphical assistance.

Supporting Information Available: Tables containing geometries and vibrational frequencies of phosphate ion and phosphate ion−water clusters and total energies of mono-, di-, and trianions. This material is available free of charge via the Internet at http://pubs.acs.org.

References and Notes

(1) Richens, D. T. *The Chemistry of Aqua Ions*; Wiley: Chichester, U.K., 1997.

(2) Michels, M. R.; Enright, T. G.; Tomney, M. R.; Pye, C. C.; Rudolph, W. W. *Can. J. Anal. Sci. Spectrosc.* **2003**, *48*, 64−76 and references 7−18 therein.

(3) For some publications of other researchers, see: (a) Armunanto, R.; Schwenk, C. F.; Rode, B. M. *J. Phys. Chem. A* **2003**, *107*, 3132−3138. (b) Spangberg, D.; Rey, R.; Hynes, J. T.; Hermansson, K. *J. Phys. Chem. B* **2003**, *107*, 4470−4477. (c) Egorov, A. V.; Komolkin, A. V.; Chizhik, V. I.; Yushmanov, P. V.; Lyubartsev, A. P.; Laaksonen, A. *J. Phys. Chem. B* **2003**, *107*, 3234−3242. (d) Koizumi, H.; Larsen, M.; Armentrout, P. B.;

Feller, D. *J. Phys. Chem. A* **2003**, *107*, 2829−2838. (e) Bock, C. W.; Markham, G. D.; Katz, A. K.; Glusker, J. P. *Inorg. Chem.* **2003**, *42*, 1538−1548. (f) Martinez, J. M.; Pappalardo, R. R.; Sanchez Marcos, E.; Mennucci, B.; Tomasi, J. *J. Phys. Chem. B* **2002**, *106*, 1118−1123.

(4) Pye, C. C.; Rudolph, W. W. *J. Phys. Chem. A* **2001**, *105*, 905−912.

(5) Rudolph, W., Ph.D. Thesis (in German), Technical University of Dresden, Dresden, Germany, 1986.

(6) Frisch, M. J.; Trucks, G. W.; Head-Gorden, M.; Gill, P. M. W.; Wong, M. W.; Foresman, J. B.; Johnson, B. G.; Schlegel, H. B.; Robb, M. A.; Replogle, E. S.; Gomperts, R.; Andres, J. L.; Rahavachari, K.; Binkley, J. S.; Gonzalez, C.; Martin, R. L.; Fox, D. J.; Defrees, D. J.; Baker, J.; Stewart, J. J. P.; Pople, J. A. *Gaussian 92*, revision F.4; Gaussian, Inc.: Pittsburgh, PA, 1992.

(7) For C−F, 6-31G: Hehre, W. J.; Ditchfield, R.; Pople, J. A. *J. Chem. Phys.* **1972**, *56*, 2257−2261. For H, C−F polarization functions: Hariharan, P. C.; Pople, J. A. *Theor. Chim. Acta (Berlin)* **1973**, *28*, 213−222. For Li−B: Dill, J. D.; Pople, J. A. *J. Chem. Phys.* **1975**, *62*, 2921−2923. For Na−Ar: Francl, M. M.; Pietro, W. J.; Hehre, W. J.; Binkley, J. S.; Gordon, M. S.; Defrees, D. J.; Pople, J. A. *J. Chem. Phys.* **1982**, *77*, 3654−3665.

(8) For H, Li−F diffuse: Clark, T.; Chandrasekhar, J.; Spitznagel, G. W.; v. R. Schleyer, P. *J. Comput. Chem.* **1983**, *4*, 294−301. For Na−Cl diffuse: Frisch, M. J.; Pople, J. A.; Binkley, J. S. *J. Chem. Phys.* **1984**, *80*, 3265−3269.

(9) Simon, A.; Schulze, G. *Z. Anorg. Allg. Chem.* **1939**, *242*, 313−369.

(10) Mathieu, J. P.; Jacques, J. *C. R. Hebd. Seances Acad. Sci.* **1942**, *215*, 346−347.

(11) Hanwick, T. J.; Hoffman, P. O. *J. Chem. Phys.* **1949**, *17*, 1166.

(12) Herzberg, G. *Molecular Structure and Molecular Spectra II, Infrared and Raman spectra of Polyatomic Molecules*; D. Van Nostrand: Princeton, NJ, 1953.

(13) Nakamoto, K. *Infrared Spectra of Inorganic and Coordination Compounds*; Wiley: New York, 1963.

(14) Robinson, E. A. *Can. J. Chem.* **1963**, *41*, 173−179.

(15) Baldwin, S. F.; Brown, C. W. *Water Res.* **1972**, *6*, 1601−1604.

(16) Preston, C. M.; Adams, W. A. *J. Phys. Chem.* **1979**, *83*, 814−821.

(17) Dean, W. *J. Raman Spectrosc.* **1983**, *18*, 22.

(18) Steger, E.; Herzog, K. *Z. Anorg. Allg. Chem.* **1964**, *331*, 169−182.

(19) Rustad, J. R.; Dixon, D. A.; Kubicki, J. D.; Felmy, A. R. *J. Phys. Chem. A* **2000**, *104*, 4051−4057.

(20) Niaura, G.; Gaigalas, A. K.; Vilker, V. L. *J. Phys. Chem. B* **1997**, *101*, 9250−9262.